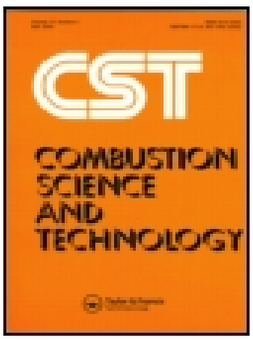

Taylor & Francis
Taylor & Francis Group

Combustion Science and Technology

ISSN: 0010-2202 (Print) 1563-521X (Online) Journal homepage: http://www.tandfonline.com/loi/gcst20

Numerical investigation on detonation control using a pulse hot jet in supersonic combustible mixture

Xiaodong Cai, Jianhan Liang & Ralf Deiterding

To cite this article: Xiaodong Cai, Jianhan Liang & Ralf Deiterding (2016): Numerical investigation on detonation control using a pulse hot jet in supersonic combustible mixture, Combustion Science and Technology, DOI: 10.1080/00102202.2016.1193499

To link to this article: http://dx.doi.org/10.1080/00102202.2016.1193499

Accepted author version posted online: 07 Jun 2016.
Published online: 07 Jun 2016.

Numerical investigation on detonation control using a pulse hot jet in supersonic combustible mixture

Xiaodong Cai[a], Jianhan Liang[a,*], Ralf Deiterding[b]

[a] Science and Technology on Scramjet Laboratory, National University of Defense Technology, 410073, Hunan Changsha.

[b] Aerodynamics and Flight Mechanics Research Group, University of Southampton, Highfield Campus, Southampton SO17 1BJ, United Kingdom

Abstract: To investigate the mechanism of detonation control using a pulse hot jet in the supersonic hydrogen-oxygen mixture, high-resolution simulations with a detailed reaction model were conducted using an adaptive mesh refinement method. After the successful detonation initiation, a contractive passway was generated between the hot jet and the main flow field behind the detonation front. Due to the contractive passway, the expansion of detonation products was prevented, hence resulting in overdriven detonation. By setting up various contractive passways through adjusting the width of the hot jet, the overdrive degree of overdriven detonation also changes. It is suggested that the width of the hot jet has approximately linear relation with the relative and absolute propagation velocities. When the contractive passway gradually disappeared after the shutdown of the hot jet, overdriven detonation attenuated to the dynamically stable Chapman-Jouguet (CJ) detonation. When the contractive passway was re-established once again after the re-injection of the hot jet, the CJ detonation developed to the same overdriven detonation, indicating that the contractive passway controlled by the pulse hot jet can indeed control detonation propagation in the

Corresponding author. Email addresses: cai-chonger@hotmail.com, jhleon@vip.sina.com, r.deiterding@soton.ac.uk, linzy96@nudt.edu.cn

supersonic combustible mixture to some extent.

Key words: detonation control, supersonic combustible mixture, hot jet, contractive passway, adaptive mesh refinement

1. Introduction

Scramjet has become one of the first choices for hypersonic air-breathing propulsion systems because of its superior performance at high Mach numbers (Murthy and Curran, 1991). Scramjet operates on the Brayton cycle, which has a much lower thermodynamic efficiency than that of detonation (Kailasanath, 2000). If a full or even a local detonation is realized in supersonic combustible mixtures in scramjet combustors, it is expected that the performance of scramjet engines might be greatly improved.

As for initiation method, direct initiation (Zhang et al., 2011a; Zhang et al., 2011b; Zhang et al., 2012; Soury and Mazaheri, 2009) can realize instantaneously detonation formation, but it is not suitable for actual application due to its requirement for large energy. An alternative approach is to use a hot jet, which can also realize fast initiation (Knystautas et al., 1979). Hot jet initiation has been investigated numerously (Medvedev et al., 2005; Liu et al., 2012; Iglesias et al., 2012); yet, only a few studies have been carried out in supersonic combustible mixtures. Ishii et al. (Ishii et al., 2009) investigated experimentally detonation initiation and propagation using a hot jet in high-speed combustible flows where the Mach numbers are 0.9 and 1.2. Han et al. (Han et al., 2012; Han et al., 2013) conducted experiments of detonation initiation and deflagration to detonation transition (DDT) using a hot jet in supersonic combustible mixtures with the Mach number above 4.0, and detonations

were initiated exactly through shocks or shock reflections (Gamezo et al., 2008; Jackson and Shepherd, 2008; Gavilanes et al., 2011; Gavilanes et al., 2013; Chaumeix et al., 2014; Liu et al., 2015).

For detonation simulations, the small area in the vicinity of detonation front is in great need of fine mesh because of accumulated chemical reactions, while the other areas could be resolved with relatively coarser grid in order to obtain a higher computational efficiency. Dynamic adaptive mesh refinement method can address this problem properly by greatly improving the local resolution while decreasing the total computational cost.

Based on these ideas above, we conducted a series of numerical simulations on detonation initiation and propagation using a hot jet in supersonic combustible mixtures (Cai et al., 2015a; Liang et al., 2014; Cai et al., 2014; Cai et al., 2015b; Cai et al., 2016a; Cai et al., 2016b) with the open-source program AMROC (Deiterding, 2003; Liang et al., 2007; Deiterding, 2009; Deiterding, 2011; Ziegler et al., 2011) (Adaptive Mesh Refinement Object-oriented C++) based on a SAMR (Structured Adaptive Mesh Refinement) framework proposed by Berger and Oliger (Berger, 1982; Berger and Oliger, 1984). These numerical simulations solved inviscid two-dimensional and three-dimensional Euler equations both with a simplified reaction model (Liang et al., 2007) and a detailed reaction model (Westbrook, 1982), and applied a classical second-order accurate MUSCL-TVD (Monotone Upstream-centered Schemes for Conservation Laws - Total Variation Diminishing) scheme. Initially we explored the probability of detonation initiation and propagation in supersonic combustible mixtures using a hot jet through two-dimensional simulations with the simplified five-step five-species reaction model. It was found that a hot jet can initiate detonation

successfully in supersonic combustible mixtures and finally overdriven detonation is formed with the continuous injection of the hot jet (Cai et al., 2015a). Subsequently, we conducted a systematic research on different effects of a hot jet to show its functions in detonation initiation and propagation, and found that through the re-injection of the hot jet a failed detonation can be re-established again quickly (Liang et al., 2014). It is necessary to know clearly the characteristics of detonation initiation in supersonic combustible mixtures using a hot jet under different conditions. Instead of the simplified reaction model, we adopted the detailed one to conduct a systematic parametric study for the characteristics of detonation initiation using a hot jet. These parameters were based on momentum flux ratios and the strength of shock reflections, and eventually ranges of different parameters for successful initiation were obtained (Cai et al., 2014). In addition, considering the actual flight conditions the velocity and species nonuniformities were investigated for detonation initiation and propagation in supersonic combustible mixtures (Cai et al., 2015b; Cai et al., 2016b). It was found that in the flowfield with nonuniform velocities there exists a wider range of Mach number of supersonic combustible mixtures for successful initiation compared with uniform supersonic incoming flow (Cai et al., 2015b). And a dynamically periodical structure of the lateral expansion of the detonation is formed finally in the flowfield with nonuniform species (Cai et al., 2016b). Finally, a study of large-scale three-dimensional simulations on detonation initiation and propagation in supersonic combustible mixtures using the detailed reaction model was conducted in Tianhe-2 supercomputer system to investigate real three-dimensional effects, especially the side wall effects (Cai et al., 2016a).

In the previous studies, it is commonly found that after detonation initiation is successfully realized overdriven detonation can be generated with the continuous injection of a hot jet in supersonic combustible mixtures. It is indicated that the hot jet can play a control role in the formation of overdriven detonation, but its mechanism is still not well understood. What's more, in order to produce stable thrust in detonation-based engines detonations should be sustained in supersonic reactive flows. However, this issue is quite difficult to address due to the internal characteristics of detonations. Rather few studies have been conducted on this issue. Previously Alexandrov et al. (Alexandrov et al., 2001; Alexandrov et al., 2003) tried to control the sustainment of oscillating detonations in supersonic reactive flows by periodical alternations of mixing ratios of combustible mixtures in Supersonic Pulsed Detonation Ramjet Engine (SPDRE). It revealed a novel and promising prospect for the sustainment control of detonation combustion in supersonic combustible mixtures. However, one of the key techniques involves the periodic control of the fuel supply system, and detonation may fail if the fuel supply is not matched properly. This issue is difficult to address in real applications. In contrast, the hot jet is easy to control through openness and shutdown. After the control role of the hot jet in overdriven detonation is investigated, the hot jet will be tried in the sustainment control of detonation wave in supersonic reactive flows.

The plan of the paper is as follows: the computational method is presented in Section 2, including the introduction of the computational model and numerical method. Results and analysis are shown in Section 3, in which the mechanism for the formation of overdriven detonation is discussed and applications of the contractive passway controlled by the hot jet are investigated. Finally Section 4 concludes the paper.

2. Computational method

2.1 Computational model

The reactive Euler equations for multiple thermally perfect species are used as governing equations, which read

$$\partial_t \rho_i + \nabla \cdot (\rho_i \vec{u}) = W_i \dot{\omega}_i \quad (1)$$

$$\partial_t (\rho \vec{u}) + \nabla \cdot (\rho \vec{u} \otimes \vec{u}) + \nabla p = 0 \quad (2)$$

$$\partial_t (\rho E) + \nabla \cdot ((\rho E + p)\vec{u}) = 0 \quad (3)$$

with $i = 1,\ldots,K$. Provided that all K species are ideal gases in the state of thermal equilibrium and the hydrostatic pressure satisfies the Dalton's Law, given as the sum of partial pressures $p_i = RT\rho_i / W_i$ with R denoting the universal gas constant and W_i the corresponding molecular weight, respectively. The evaluation of Equation 3 requires iterative calculation of temperature T. A time operator splitting approach is employed to decouple numerically the hydrodynamic transport and chemical reaction. Temperature-dependent material properties are taken from look-up tables that are constructed during the start of the computational code. The reaction rates are evaluated by a Fortran-77 function, which is produced by a source code generator on top of the Chemkin-II library in advance.

Numerical simulations are conducted in a straight channel, as shown in Fig.1. Reflecting boundaries with slip wall conditions are used on the upper and lower wall, except for a small inflow embedded into the lower wall which models a hot jet. The right boundary models the inflow condition and the left one the ideal outflow condition. Based on the regularity of cellular detonation structure (Shepherd, 2009; Radulescu et al., 2007; Gamezo et al., 1999;

Mach and Radulescu, 2010; Hu et al., 2004; Mahmoudi and Mazaheri, 2012), numerical and experimental investigations (Mahmoudi and Mazaheri, 2011; Radulescu and Lee, 2002; Radulescu et al., 2005) indicate the existence of two kinds of detonation structures which are classified as regular (weakly unstable) and irregular (highly unstable) detonations. Self-sustaining CJ detonations in hydrogen-oxygen mixtures with high-argon dilution in low pressure are ideal candidates for detonation simulations because regular detonation cell patterns can be generated (Strehlow, 1968). The channel consists of H_2/O_2/Ar mixture with a molar ratio 2:1:7, and the initial pressure and temperature are 6.67 kPa and 298 K, respectively. The propagating speed of the mixture is given by the corresponding CJ velocity (referenced $V_{CJ} = 1627$ m/s).

When dealing with the hot jet condition, the parameter "time" is considered to control the duration of the hot jet injection. When the hot jet is shut down, the inflow condition is switched immediately to the reflecting boundary condition. Here as shown in Table 1, we set the inflow parameters of the hot jet to the equilibrium CJ state of H_2/O_2 with a molar ratio of 2:1 under the condition of pressure 6.67 kPa and temperature 298 K, which is calculated with Cantera (Goodwin, 2001).

2.2 Numerical method

A second-order accurate MUSCL-TVD finite volume method (FVM) is adopted for discretization. The difference between considering the reaction source term with the first-order accurate Godunov splitting or the second-order accurate Strang splitting is usually small (Deiterding, 2003), therefore the computationally more efficient Godunov splitting

method is employed here. A hybrid Roe-HLL (Deiterding, 2003) Riemann solver is used to construct the inter-cell numerical upwind fluxes, the Van Albada limiter with MUSCL reconstruction is applied to construct a second-order method in space, and the MUSCL-Hancock technique (Leer, 1984) is adopted for second-order accurate time integration.

The comparison between inviscid and viscous detonations is an interesting point. For simulations using shock-capturing methods, numerical diffusion is determined by grid resolution (Sharpe, 2001). At low grid resolution solutions of Euler and Navier-Stokes (NS) equations are similar because numerical diffusion dominates over physical diffusion. When grid resolution increases, numerical diffusion decreases and physical diffusion dominates over numerical diffusion. An excellent discussion of this issue is provided by Samtaney and Pullin (Samtaney and Pullin, 1996). In high grid resolution, detonation simulations using Euler equations can generate unphysical small-scale features resulting from low numerical diffusion. However, even in high grid resolution qualitative agreement is obtained in detonation simulations by solving Euler and NS equations, especially for regular detonations. Previously Oran et al. (Oran et al., 1998) performed a series of detonation simulations using both Euler and NS equations with detailed chemical kinetics, and observed similar structures of stable detonations for both Euler and NS equations. They indicated that small-scale structures that are eliminated in Euler computations do not affect the overall features of stable detonations. Recent numerical investigations (Mazaheri et al., 2012; Mahmoudi et al., 2013; Mahmoudi et al., 2014) showed that from the comparison between Euler and NS equations, diffusion effect has no role in regular detonations, due to the absence of hydrodynamic

instabilities (Kelvin-Helmholtz (K-H) instability and Richtmyer-Meshkov (R-M) instability). Therefore, the conclusions obtained in this paper using the inviscid Euler equations for regular detonations are nevertheless expected to give at least qualitatively correct descriptions of detonation features.

3. Results and Analysis

As shown in Fig.1, the height and length of the channel are Y_1 = 3 cm and X_1 = 8 cm. The hot jet with the width of X_3 = 4.0 mm, is X_2 = 4.5 cm away from the left outflow of the channel. The detonation cellular size under the given conditions is $\lambda = 3\,\mathrm{cm}$, so the geometry setup allows the development of a full detonation cell in the Y direction. The initial mesh is 320×80, and the induction length of the ZND model is $l_{ig} = 1.509\,\mathrm{mm}$. For the adopted five-level mesh refinement with the corresponding refinement factors $r_1 = 2,\ r_2 = 2,\ r_3 = 2,\ r_4 = 2$, the final resolution can be as high as $96.8\,Pts/l_{ig}$, which is the same as that in the previous work (Cai et al., 2015b). All the computations are conducted on a parallel cluster using 72 nodes of Intel Xeon X5675-3.06 GHz.

3.1 Formation of overdriven detonation

The detailed process of detonation initiation in the supersonic combustible mixture using a hot jet has been shown (Cai et al., 2014). Here, a brief illustration is provided for a quick understanding of this issue, as shown in Fig.2. After the hot jet is injected into the channel, a bow shock is induced in the supersonic incoming flow, as shown in Fig.2(a). The shock wave becomes stronger gradually and eventually reflects on the upper wall. After the reflection, a

Mach reflection is formed due to the enhanced strength of the shock wave, as shown in Fig.2(b). Compared with Fig.2(b), the Mach stem in Fig.2(c) has propagated forward obviously. After the Mach stem reaches the lower wall, a second reflection is generated as an ignition source, which can help to realize detonation initiation successfully. With the continuous injection of the hot jet, detonation propagates forward continuously as shown in Fig.2(d).

It should be noted that, in this simulation a straight Mach stem perpendicular to the upper wall is generated following with an obviously slip line which gradually developed to unstable shear layer because of K-H instability. This is different from the previous work (Cai et al., 2015a). As shown in Fig.3(a), behind the Mach stem is the reaction zone which is visualized by the contour of OH radical mass fraction. In Fig.3(b), it is calculated that the distance between the reaction front and the Mach stem is about 1.0 mm, only 67% of the induction length of the ZND model (l_{ig} = 1.509 mm). The Mach stem is coupled tightly with the reaction zone behind, indicating that the Mach stem here is actually a local Mach detonation. The formation of the local Mach detonation near the upper wall plays a critical role in the successful detonation initiation. However, in (Cai et al., 2015a) where the simulations are conducted with the simplified reaction model and a coarser spatial resolution, a local detonation is realized first in front of the hot jet. Subsequently another local detonation is formed on the upper wall because of the strengthened bow shock enhanced by the local detonation near the lower wall.

As shown in Fig.4, detonation spreads throughout the entire channel during the latter period, which can be proven to be actually an overdriven detonation (Liang et al., 2014).

Numerical density schlieren images are obtained by calculating the square root of density gradients in X and Y directions. The cellular size under the given condition is $\lambda \cong 3\,\mathrm{cm}$, therefore for the CJ detonation in the channel with the height of Y_1 = 3 cm, one regular detonation cell should be generated. Fig.4 shows the typical structure of an overdriven detonation which has more cells than a CJ detonation. In Fig.4(a)(b) almost three cells can be observed. The propagation velocity of overdriven detonation is larger than the CJ velocity, therefore the strength of its detonation front is stronger than that of the corresponding CJ detonation, which results in a faster release rate of chemical heat behind the detonation front. Because the transverse waves are determined by the heat release, the transverse waves can propagate faster due to faster release rate of chemical heat and thus more triple points and detonation cells are generated.

3.2 Mechanism of contractive passway

The formation of overdriven detonation has been proven already, but it is still not well understood how overdriven detonation is generated in substance. Behind the detonation front there exists a slip shear layer associated with large-scale vortices due to K-H instability, which generates an interface between the hot jet and the main flow field and helps to form a contractive passway, as shown in Fig.5. The velocity vector images show that the direction of the flow field in the vicinity of the hot jet changes owing to the contractive passway. Therefore, the expansion of detonation products is prevented to some extent because of the contractive passway, hence resulting in pressure increase behind the detonation front. The pressure curves at X = 4.9 cm along the Y direction at four successive times are depicted in

Fig.6, which shows that the pressures at X = 4.9 cm along the Y direction are all larger than P_{CJ}. The highest pressure is nearly two times of P_{CJ}, and even the smallest pressure is 35.84% higher than P_{CJ}. All the four curves with a similar shape and variation range have approximately the same trend of decreasing gradually along the Y direction. Therefore, the detonation front has to propagate toward the supersonic incoming flow to increase the relative Mach number for pressure matching, hence finally resulting in the overdriven detonation.

On the other side, due to the expansion prevention resulting from the contractive passway, the acceleration of detonation products is also prevented from reaching the sonic speed. During the products expansion, the Mach number of the products behind the detonation front increases gradually. However, it is shown in Fig.7 that the flow field is all subsonic between the front of the hot jet and the detonation front, indicating that because of the contractive passway the flow field cannot accelerate to the sonic speed, which is a CJ condition of the CJ theory. On the contrary, there exists a supersonic zone behind the hot jet. As shown in Fig.8, the flowfield behind the detonation front is similar to that of Laval nozzle, where three different velocity zones are formed. Owing to the compression of products expansion on the shear layer which can be regarded as a free boundary, a slightly expanded channel is generated in the downstream of the hot jet, and therefore detonation products can expand to the supersonic speed.

3.3 Validation of contractive passway

Since it is suggested that overdriven detonation results from the contractive passway and the contractive passway is generated by the injection of the hot jet, a series of numerical experiments are conducted for verification. Here only the width of the hot jet is changed while keeping all the other conditions the same. Four different widths of hot jets are shown as follows: D1 = 4.0 mm between [4.5, 4.9] cm; D2 = 4.25 mm between [4.5, 4.925] cm; D3 = 4.5 mm between [4.5, 4.95] cm; D4 = 5.0 mm between [4.5, 5.0] cm. These hot jets with different widths can all successfully realize detonation initiation (Cai et al., 2014). The four curves in Fig.9 are all almost straight lines, where the slopes of the lines denote the relative propagating velocities. The corresponding speeds and overdrive degrees for the four different widths of hot jets are shown in Table 2, where $f = (1 + u/V_{CJ})^2$. According to Table 2, it is suggested that

$$\frac{\text{D2-D1}}{u_2 - u_1} \cong \frac{\text{D3-D2}}{u_3 - u_2} \cong \frac{\text{D4-D3}}{u_4 - u_3} \tag{4}$$

$$\frac{\text{D2-D1}}{V_2 - V_1} \cong \frac{\text{D3-D2}}{V_3 - V_2} \cong \frac{\text{D4-D3}}{V_4 - V_3} \tag{5}$$

It is indicated from Equation 4 and 5 that the width of the hot jet has approximately a linear relation with the relative and absolute propagation velocities of detonations. Hot jets with different widths can result in variations of the contractive passway, and therefore when the hot jet width becomes larger, the passway behind the detonation front will become more contractive, thus making the detonation more overdriven.

3.4 Application of contractive passway

The contractive passway resulting from the hot jet plays an important role in detonation propagation, as discussed previously. Therefore, detonation control can be realized to some extent in the supersonic combustible mixture by changing the contractive passway through the control of the hot jet. During the propagation of overdriven detonation the same hot jet for the two cases is shut down at $t_{sd} = 400\ \mu s$ and $t_{sd} = 440\ \mu s$, respectively. When the hot jet is shut down, the contractive passway produced by the hot jet vanishes gradually. As shown in Fig.10, the slopes of the two curves both decrease after the shutdown of the hot jet, indicating that the two overdriven detonations are attenuating and overdrive degrees are decreasing along with the gradual disappearance of contractive passways. Finally, dynamically stable states are formed both for the two cases at approximately the same velocity at $t = 720\ \mu s$ for $t_{sd} = 400\ \mu s$ and $t = 770\ \mu s$ for $t_{sd} = 440\ \mu s$, respectively. The final stable state for $t_{sd} = 440\ \mu s$ is shown in Fig.11, and the detonation structures are quite similar to the experimental images of CJ detonation for $H_2/O_2/Ar$ mixture presented by Pintgen et al. (Pintgen et al., 2003), indicating that the final dynamically stable state is CJ detonation. The relative propagating velocity of the CJ detonation is $u = -36.69$ m/s, and then the absolute velocity is $\bar{V}_{CJ} = V_{CJ} + u = 1590.31$ m/s with a relative error $\varepsilon = 2.25\%$ ($\varepsilon = \frac{V_{CJ} - \bar{V}_{CJ}}{V_{CJ}}$) with the referenced CJ velocity in this case. It should be noted that it is quite different here from the result solved with the simplified reaction model, where the overdriven detonation gradually attenuates and finally fails after the shutdown of the hot jet. In the previous investigation, it is suggested if the overdrive

degree does not reach the stable value before the shutdown of the hot jet, detonation will finally fail. However, it is not this case here. For the case here when the hot jet is shut down at $t_{sd} = 400\ \mu s$, the overdrive degree does not reach the final stable value either, but overdriven detonation does not decouple and finally attenuates successfully to the CJ detonation. The simplified reaction model may have led to the loss of fine features usually characterized by complex chain-branching reactions, which might have an influence on detonation evolution. For the high resolution here, only when simplified multi-step reaction model is reduced carefully can it probably get results close to that using detailed reaction model.

As shown in Fig.12, when the hot jet is injected into the channel again at $t = 900\ \mu s$, the CJ detonation changes to overdriven detonation once again because of reformation of the contractive passway. It is indicated that the newly formed overdriven detonation in stage D has almost the same overdrive degree as stage A, because the same contractive passway is generated in the flowfield after the re-injection of the same hot jet. This numerical experiment of the hot jet re-injection proves that the contractive passway generated by the hot jet actually plays an important role in detonation control in the supersonic combustible mixture.

3.5 Convergence analysis for mesh refinement

In the ZND solution it is found that for the realistic reaction considered here, a spatial resolution of minimally $6\,Pts/l_{ig}$ is necessary to resolve all intermediate reaction products accurately (Deiterding, 2005). However, around multi-dimensional triple points a higher

resolution is required to capture the internal wave structure completely. For regularly oscillating detonations, the effective resolution up to $44.8\ Pts/l_{ig}$ is used in the previous two-dimensional verification simulations which indicate that this resolution is sufficient for resolving reliably even the secondary triple point (Deiterding, 2003). Here three different distributions of mesh refinement are shown in Fig.13, where the resolutions are all higher than $44.8\ Pts/l_{ig}$. In the flowfield, the same pattern for the Mach reflection, bow shock, and shock induced combustion is all presented for the three different cases, and especially all are covered by the highest levels (the red color). As a comprise of the accuracy and computational cost, the second highest resolution $96.8\ Pts/l_{ig}$ in Fig.13(b) is chosen finally.

4. Conclusion

Based on an adaptive mesh refinement method, detonation control mechanism in the supersonic combustible mixture was investigated using a pulse hot jet through two-dimensional high-resolution simulations with a detailed reaction model. The major results of the present work are as follows:

1. After the successful detonation initiation, a contractive passway is generated between the hot jet and the main flowfield behind the detonation front due to formation of a slip shear layer which is regarded as a free boundary resulting from the hot jet. The contractive passway prevents the expansion of detonation products, and the detonation front has to propagate forward for pressure matching, hence resulting in overdriven detonation.
2. By setting up various contractive passways through adjusting the width of the hot jet,

the overdrive degree of overdriven detonation also changes. When the hot jet width becomes larger, the passway behind the detonation front becomes more contractive, thus making the detonation more overdriven. On the other hand, when the hot jet width becomes smaller, the passway behind the detonation front becomes less contractive, thus making the detonation less overdriven. It is suggested that the width of the hot jet has approximately a linear relation with the relative and absolute propagation velocities.

3. As an application, when the contractive passway gradually disappears after the shutdown of the hot jet, overdriven detonation attenuates to the dynamically stable CJ detonation. When the contractive passway is re-established once again through the re-injection of the hot jet, the CJ detonation changes again to the overdriven detonation with the same overdrive degree as that of the previous overdriven detonation. It is also proven that the contractive passway controlled by the pulse hot jet can indeed control detonation propagation in the supersonic combustible mixture.

5. Acknowledgements

This work is supported by National Natural Science Foundation of China (No. 51006119), and Innovative Sustentation Fund for Excellent Ph.D. Students in NUDT (No. B140101).

References

Alexandrov, V.G., Kraiko, A.N., and Reent, K.S. 2003. Integral and local characteristics of supersonic pulsed detonation ramjet engine (SPDRE). *J. Mathematical Modeling*, 15, 17-26.

Alexandrov, V.G., Kraiko, A.N., and Reent. K.S. 2001. The determination of characteristics of supersonic pulsed detonation ramjet engine (SPDRE). *J. Aeromechanics Gas Dynamics*, 2, 3-15.

Berger, M. 1982. Adaptive mesh refinement for hyperbolic differential equations, Ph.D. thesis. Stanford University, USA.

Berger, M., and Oliger, J. 1984. Adaptive mesh refinement for hyperbolic partial differential equations. *J. Comput. Phys*., 53, 484-512.

Cai X.D., Liang, J.H., Deiterding, R., Che, Y.G., and Lin, Z.Y. 2016a5c. Adaptive mesh refinement based simulations of three-dimensional detonation combustion in supersonic combustible mixtures with a detailed reaction model. *Int. J. Hydrogen Energ*., 41, 3222-3239.

Cai, X.D., Liang, J.H., Deiterding, R., Lin, Z.Y. 2016b. Numerical simulation of detonation initiation and propagation in supersonic combustible mixtures with non-uniform species. *AIAA J*.

Cai, X.D., Liang, J.H., Lin, Z.Y., Deiterding, R., and Liu, Y. 2014. Parametric study of detonation

initiation using a hot jet in supersonic combustible mixtures. *Aerosp. Sci. Technol*., 39, 442-455.

Cai, X.D., Liang, J.H., Lin, Z.Y., Deiterding, R., and Zhuang, F.C. 2015b. Detonation initiation and propagation in nonuniform supersonic combustible mixtures, *Combust. Sci. Technol*., 187, 525-536.

Cai, X.D., Liang, J.H., Lin, Z.Y., Deiterding, R., Qin, H., and Han, X. 2015a. Adaptive mesh refinement based numerical simulation of detonation initiation in supersonic combustible mixtures using a hot jet. ASCE *J. Aerosp. Eng*., 28, 04014046.

Chaumeix, N., Imbert, B., Catoire, L., and Paillard, C.E. 2014. The onset of detonation behind shock waves of moderate intensity in gas phase. *Combust. Sci. Technol*., 186, 607-620.

Deiterding, R. 2003. Parallel adaptive simulation of multi-dimensional detonation structures. Ph.D. thesis. Brandenburgische Technische Universitäat Cottbus, Germany.

Deiterding, R. 2009. A parallel adaptive method for simulating shock-induced combustion with detailed chemical kinetics in complex domains. *Comput. Struct*., 87, 769-783.

Deiterding, R. 2011. High-resolution numerical simulation and analysis of Mach reflection structures in detonation waves in low-pressure H2-O2-Ar mixtures: A summary of results obtained with the adaptive mesh refinement framework AMROC. *J. Combust*., 2011, Article ID 738969.

Deiterding, R., and Bader, G. 2005. High-resolution simulation of detonations with detailed chemistry. Springer.

Gamezo, V.N., Desbordes, D., and Oran, E.S. 1999. Formation and evolution of two-dimensional cellular detonations. *Combust. Flame*, 116, 154-165.

Gamezo, V.N., Ogawa, T., and Oran E.S. 2008. Flame acceleration and DDT in channels with obstacles: Effect of obstacle spacing. *Combust. Flame*, 155, 302-315.

Gavilanes, J.M., and Bauwens, L. 2013. Shock initiated ignition for hydrogen mixtures of different concentrations. *Int. J. Hydrogen Energ*., 38, 8061-8067.

Gavilanes, J.M., Rezaeyan, N., Tian, M., and Bauwens, L. 2011. Shock-induced ignition with single step Arrhenius kinetics. *Int. J. Hydrogen Energ*., 36, 2374-2380.

Goodwin, D. 2001. Cantera: Object-oriented software for reacting flows. Technical Report, California Institute of Technology. Available at: http://www.cantera.org.

Han, X., Zhou, J., and Lin, Z.Y. 2012. Experimental investigations of detonation initiation by hot jets in supersonic premixed flows. *Chin. Phys. B.*, 21, 124702.

Han, X., Zhou, J., and Lin, Z.Y., and Liu, Y. 2013. Deflagration-to-detonation transition induced by hot jets in a supersonic premixed airstream. *Chin. Phys. Lett*., 30, 054701.

Hu, X.Y., Khoo, B.C., Zhang, D.L., and Jiang, Z.L. 2004. The cellular structure of a two-dimensional H_2/O_2/Ar detonation wave. *Combust. Theory Model*., 8, 339-359.

Iglesias, I., Vera, M., Sánchez, A. L., and Liñán, A. 2012. Numerical analyses of deflagration initiation by a hot jet. *Combust. Theor. Model*., 16, 994-1010.

Ishii, K., Kataoka, H., and Kojima, T. 2009. Initiation and propagation of detonation waves in combustible high speed flows. *Proc. Combust. Inst*., 32, 2323-2330.

Jackson, S.I., and Shepherd, J.E. 2008. Detonation initiation in a tube via imploding toroidal shock waves. *AIAA J*., 46, 2357-2367.

Kailasanath, K. 2000. Review of propulsion applications of detonation waves. *AIAA J*., 38, 1698-1708.

Knystautas, R., Lee, J.H.S., Moen, I., and Wagner, H.G.G. 1979. Direct initiation of spherical detonation by a hot turbulent gas jet. *Seventeenth Symposium (International) on Combustion*, 17, 1235-1245.

Leer, B.V. 1984. On the relation between the upwind-differencing schemes of Godunov, EngquistOsher and Roe. *SIAM Sci. Stat. Comput*., 5, 1-20.

Liang, J.H., Cai, X.D., Lin, Z.Y., and Deiterding, R. 2014. Effects of a hot jet on detonation initiation and propagation in supersonic combustible mixtures. *Acta Astronaut*., 105, 265-277.

Liang, Z., Browne, S., Deiterding, R., and Shepherd, J.E. 2007. Detonation front structure and the competition for radicals. *Proc. Combust. Inst*., 31, 2445-2453.

Liu, S.J., Lin, Z.Y., Liu, W.D., Lin, W., and Zhuang, F.C. 2012. Experimental Realization of H_2/Air Continuous Rotating Detonation in a Cylindrical Combustor. *Combust. Sci. Technol*., 184, 1302-1317.

Liu, Y., Wu, D., Yao, S.B., and Wang, J.P. 2015. Analytical and numerical investigations of wedge-induced oblique detonation waves at low Mach number, *Combust. Sci. Technol*., 187, 843-856.

Mach, P., and Radulescu, M.I. 2010. Mach reflection bifurcations as a mechanism of cell multiplication in gaseous detonations. *Proc. Combust. Inst*., 33, 2279-2285.

Mahmoudi, Y., and Mazaheri, K. 2011. High resolution numerical simulation of the structure of 2-D gaseous detonations. *Proc. Combust. Inst*., 33, 2187-2194.

Mahmoudi, Y., and Mazaheri, K. 2012. Triple point collision and hot spots in detonations with regular structure, *Combust. Sci. Technol*., 184, 1135-1151.

Mahmoudi, Y., Karimi, N., Deiterding, R., and Emami, S. 2014. Hydrodynamic instabilities in gaseous detonations: Comparison of Euler, Navier-Stokes, and Large-Eddy simulation. *J Propul. Power*, 30, 384-96.

Mahmoudi, Y., Mazaherin, K., and Parvar, S. 2013. Hydrodynamic instabilities and transverse waves in propagation mechanism of gaseous detonations. *Acta Astronaut*., 91, 263-82.

Mazaheri, K., Mahmoudi, Y., and Radulescu, M.I. 2012. Diffusion and hydrodynamic instabilities in gaseous detonations. *Combust. Flame*, 113, 2138-2154.

Medvedev, S.P., Khomik, S.V., Olivier, H., Polenov, A.N., Bartenev, A.M., and Gelfand, B.E. 2005. Hydrogen detonation and fast deflagration triggered by a turbulent jet of combustion products. *Shock Waves*, 14, 193-203.

Murthy, S.N.B., and Curran, E.T. 1991. High-speed flight propulsion systems. *Prog. Astronaut. Aeronaut*., 137, 124-158.

Oran, E.S., Weber, J.W., Stefaniw, E.I., Lefebvre, M.H., and Anderson J.D. 1998. A numerical study of a two-dimensional H_2-O_2-Ar detonation using a detailed chemical reaction model. *Combust. Flame*, 113, 147-163.

Pintgen, F., Eckett, C.A., Austin, J.M., and Shepherd, J.E. 2003. Direct observations of reaction zone structure in propagating detonations. *Combust. Flame*, 133, 211-229.

Radulescu, M.I., and Lee, J.H.S. 2002. The failure mechanism of gaseous detonations: experiments in porous wall tubes. *Combust. Flame*, 131, 29-46.

Radulescu, M.I., Sharpe, G.J., Law, C.K., and Lee, J.H.S. 2007. The hydrodynamic structure of unstable cellular detonations. *J. Fluid Mech*., 580, 31-81.

Radulescu, M.I., Sharpe, G.J., Lee, J.H.S., Kiyanda, C.B., Higgins, A.J., and Hanson, R.K. 2005. The ignition mechanism in irregular structure gaseous detonations. *Proc. Combust. Inst.*, 30, 1859-1867.

Samtaney, R. and Pullin, D.I. 1996. On initial-value and self-similar solutions of the compressible Euler equations. *Phys. Fluids*, 8, 2650-2655.

Sharpe, G.J. 2001. Transverse waves in numerical simulations of cellular detonations. *J. Fluid Mech*., 447, 31-51.

Shepherd, J.E. 2009. Detonation in gases. *Proc. Combust. Inst*., 32, 83-98.

Soury, H., and Mazaheri, K. 2009. Utilizing unsteady curved detonation analysis and detailed kinetics to study the direct initiation of detonation in H_2-O_2 and H_2 Air mixtures. *Int. J. Hydrogen Energ*., 34, 9847-9856.

Strehlow, R.A. 1968. Gas phase detonations: Recent developments. *Combust. Flame*, 12, 81-101.

Westbrook, C.K. 1982. H2-O2-AR reaction mechanism from chemical kinetics of hydrocarbon oxidation in gaseous detonations. *Combust. Flame*, 46, 191-210.

Zhang, B., Kamenskihs, V., Ng, H.D., and Lee, J.H.S. 2011a. Direct blast initiation of spherical gaseous detonations in highly argon diluted mixtures. *Proc. Combust. Inst*., 33, 2265-2271.

Zhang, B., Ng, H.D., and Lee, J.H.S. 2012. Measurement of effective blast energy for direct initiation of spherical gaseous detonations from high-voltage spark discharge. *Shock Waves*, 22, 1-7.

Zhang, B., Ng, H.D., Mével, R., and Lee, J.H.S. 2011b. Critical energy for direct initiation of spherical detonations in H_2/N_2O/Ar mixtures. *Int. J. Hydrogen Energ*., 36, 5707-5716.

Ziegler, J.L., Deiterding, R., Shepherd, J.E., and Pullin, D.I. 2011. An adaptive high-order hybrid scheme for compressive, viscous flows with detailed chemistry. *J. Comput. Phys*., 230, 7598-7630.

Table 1 The equilibrium CJ state of H_2/O_2 with the molar ratio of 2:1 under the condition of temperature 298 K, and pressure 6.67 kPa. Note that the parameters of the nine species are given by the mass fractions.

State parameter	**Value**	**Unit**
Pressure	113585.12	Pa
Temperature	3204.8374	K
Density	0.05959	kg/m^3
Velocity	1229.9015	m/s
Energy	83445.813	J/m^3
H_2	0.024258141648492	
H	0.007952664033931	
O	0.055139351559790	
O_2	0.124622185271180	
OH	0.161144120322560	
H_2O	0.626759466258162	
HO_2	0.000117215557650	
H_2O_2	0.000006855348235	
Ar	0	

Table 2 Corresponding parameters for four different widths of hot jets

	D (mm)	u **(m/s)**	V **(m/s)**	f
Case 1	D1 = 4.0	$u_1 = 120.7$	V_1 = 1747.7	$f_1 = 1.1538$
Case 2	D2 = 4.25	$u_2 = 125.1$	V_2 = 1752.1	$f_2 = 1.1597$
Case 3	D3 = 4.5	$u_3 = 130.6$	V_3 = 1757.6	$f_3 = 1.1669$
Case 4	D4 = 5.0	$u_4 = 141.4$	V_4 = 1768.4	$f_4 = 1.1814$

List of figure captions:

Fig.1 Schematic of the calculation model

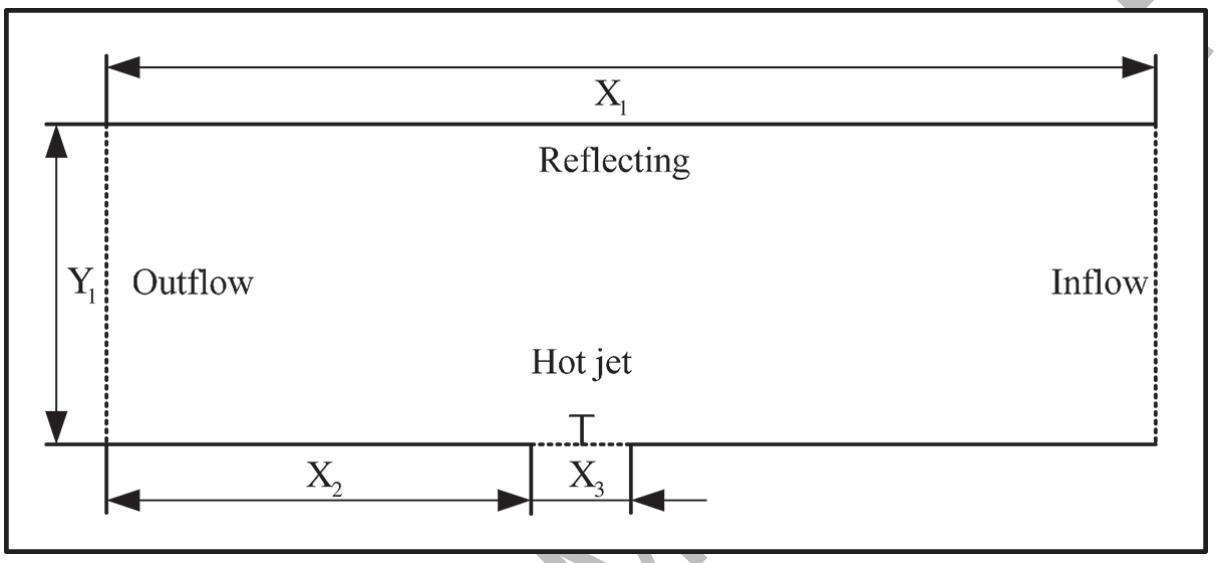

Fig.2 The process of detonation initiation in the supersonic combustible mixture, (a) t = 133.435 μs, (b) t = 198.263 μs, (c) t = 318.161 μs, (d) t = 427.439 μs

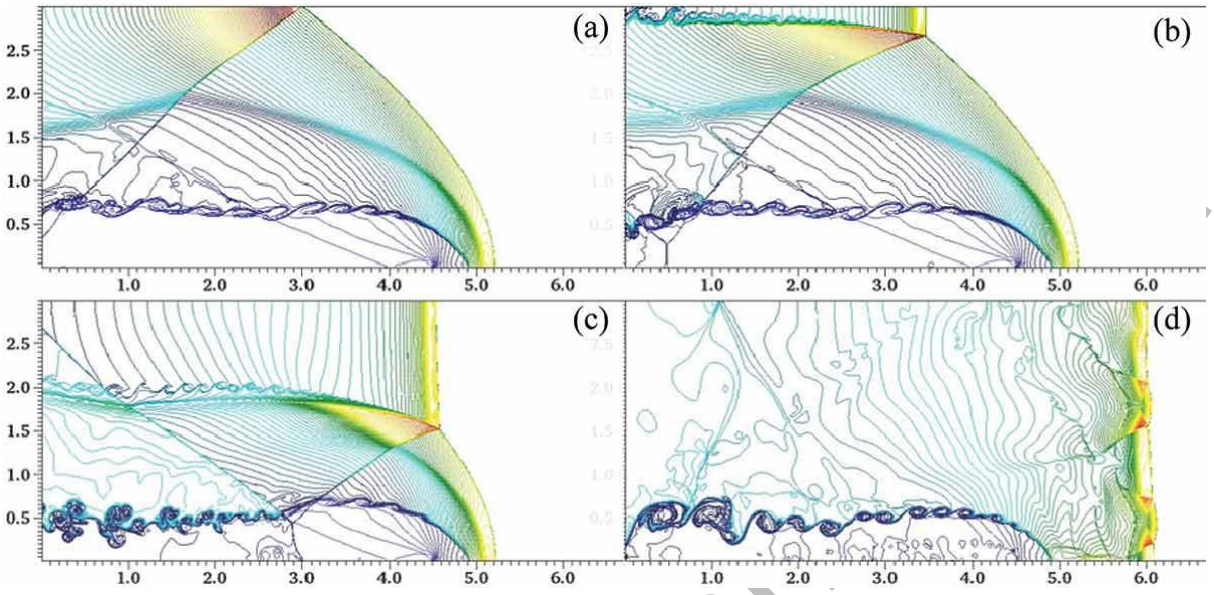

Fig.3 The triple point structure at $t = 235.7$ μs

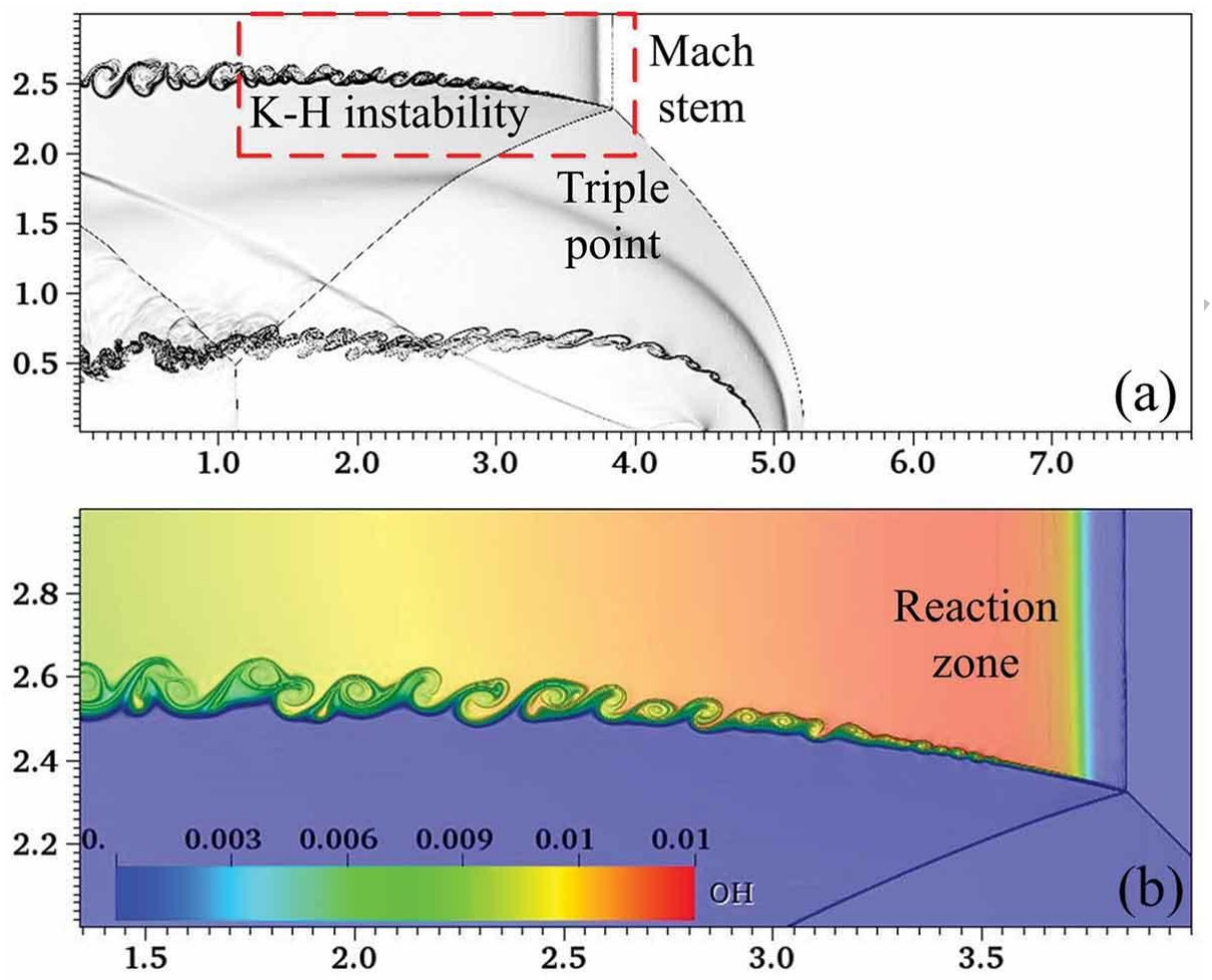

Fig.4 Density schlieren images for overdriven detonation, (a) t = 487.07 μs , (b) t = 500.01 μs

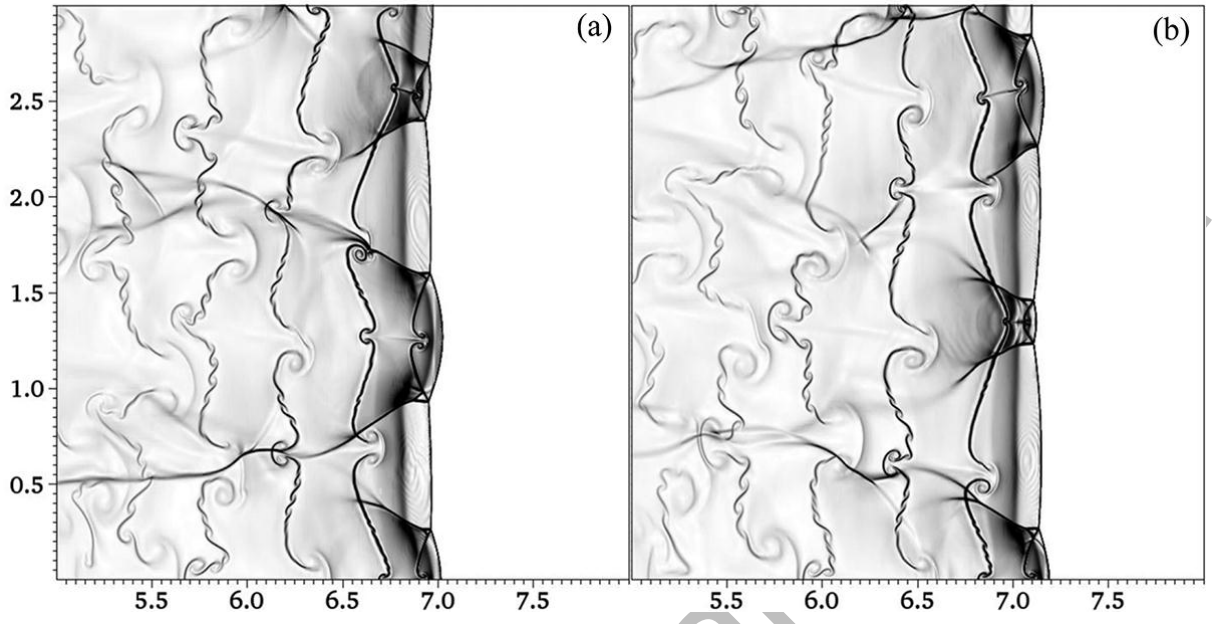

Fig.5 Contractive passway near the hot jet at $t = 408.2$ μs

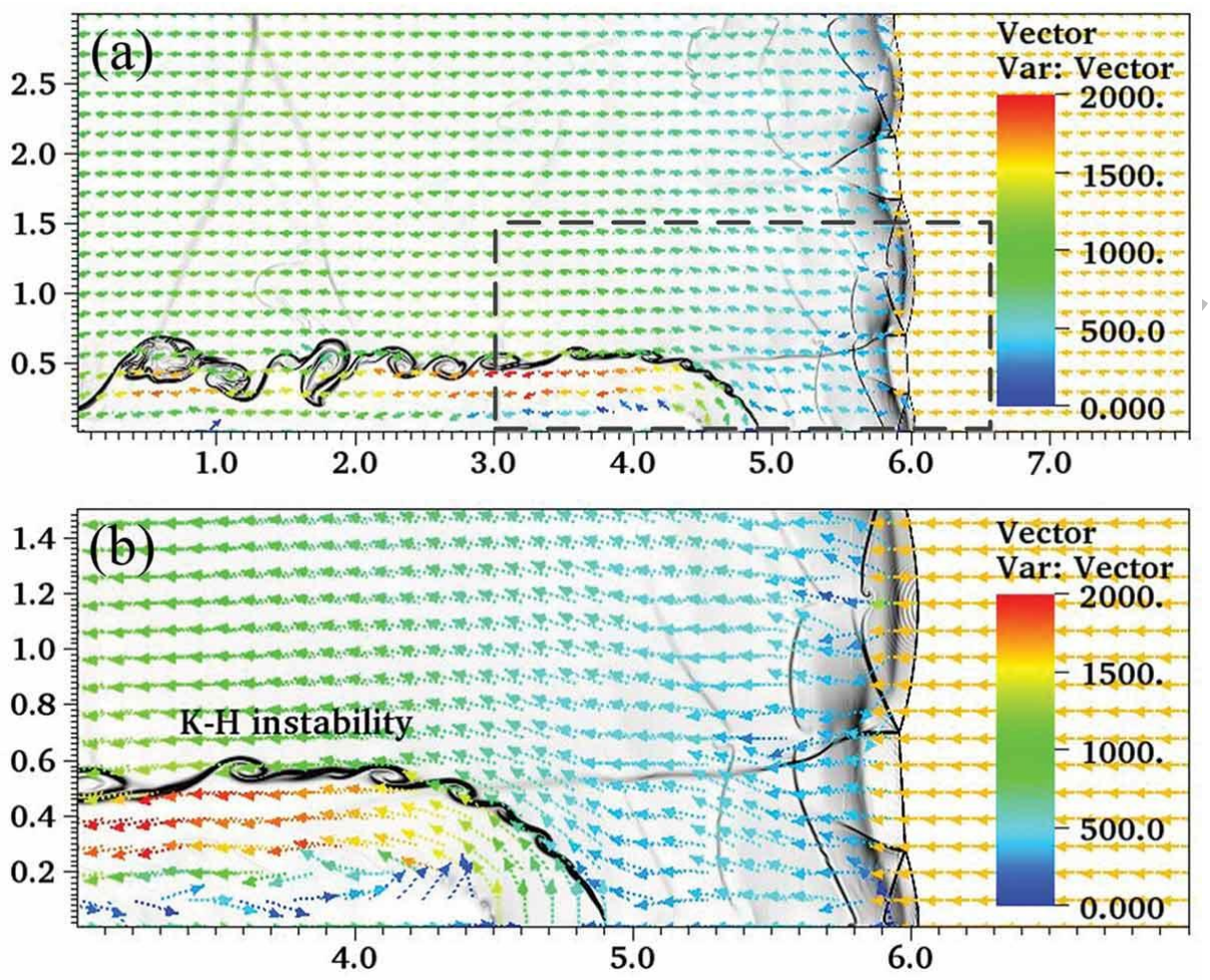

Fig.6 Pressure variations along the Y direction at X = 4.9 cm, (a) t = 414.3 μs , (b) t = 417.6 μs , (c) t = 420.9 μs , (d) t = 424.1 μs

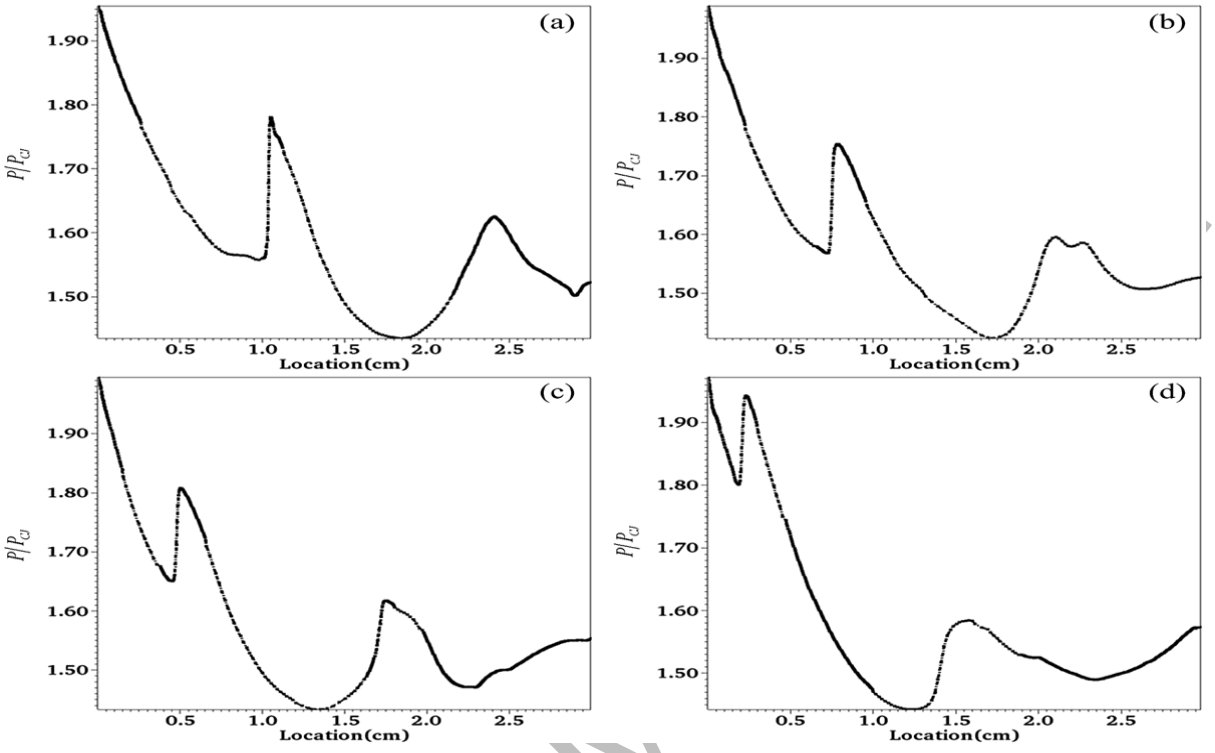

Fig.7 Contours of Mach number and sonic lines for overdriven detonation, (a) t = 411.04 μs, (b) t = 430.7 μs

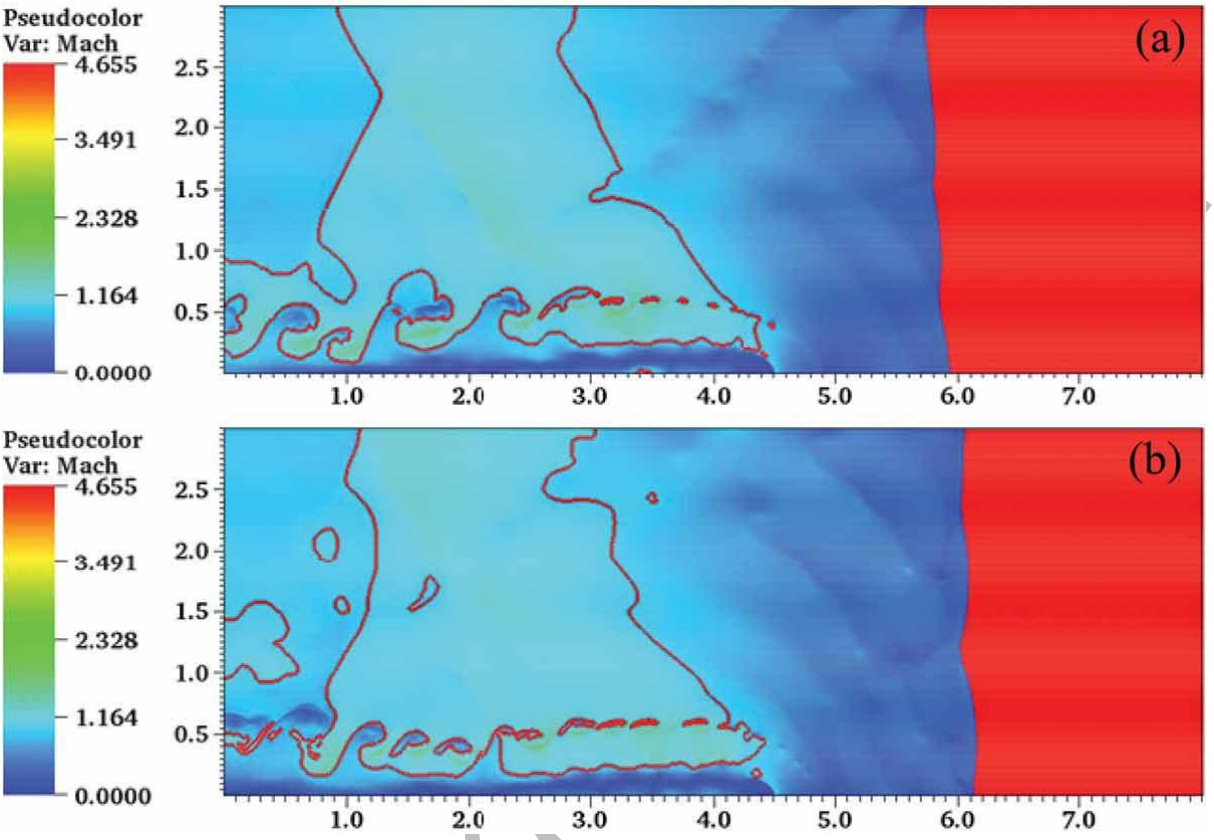

Fig.8 Schematic of the velocity flowfield behind the detonation front

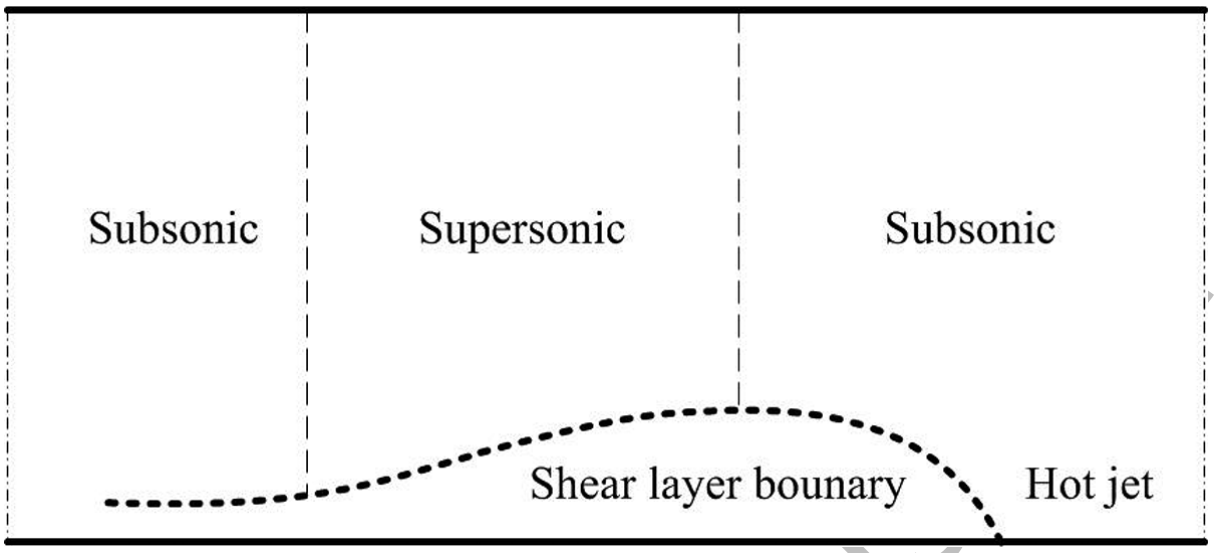

Fig.9 Detonation front locations under the continuous injection of hot jets with different widths

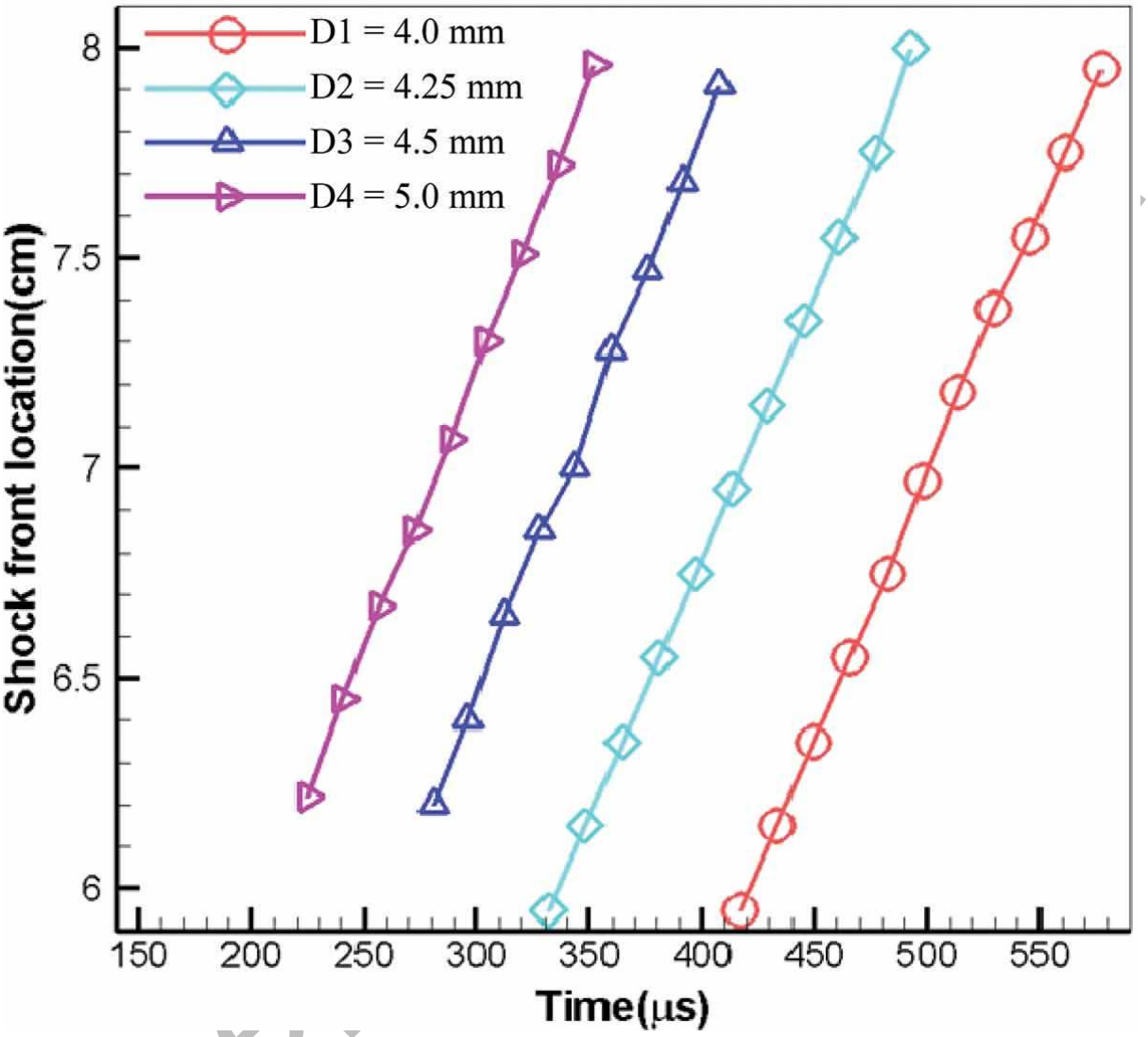

Fig.10 Detonation front locations after the shutdown of the hot jet

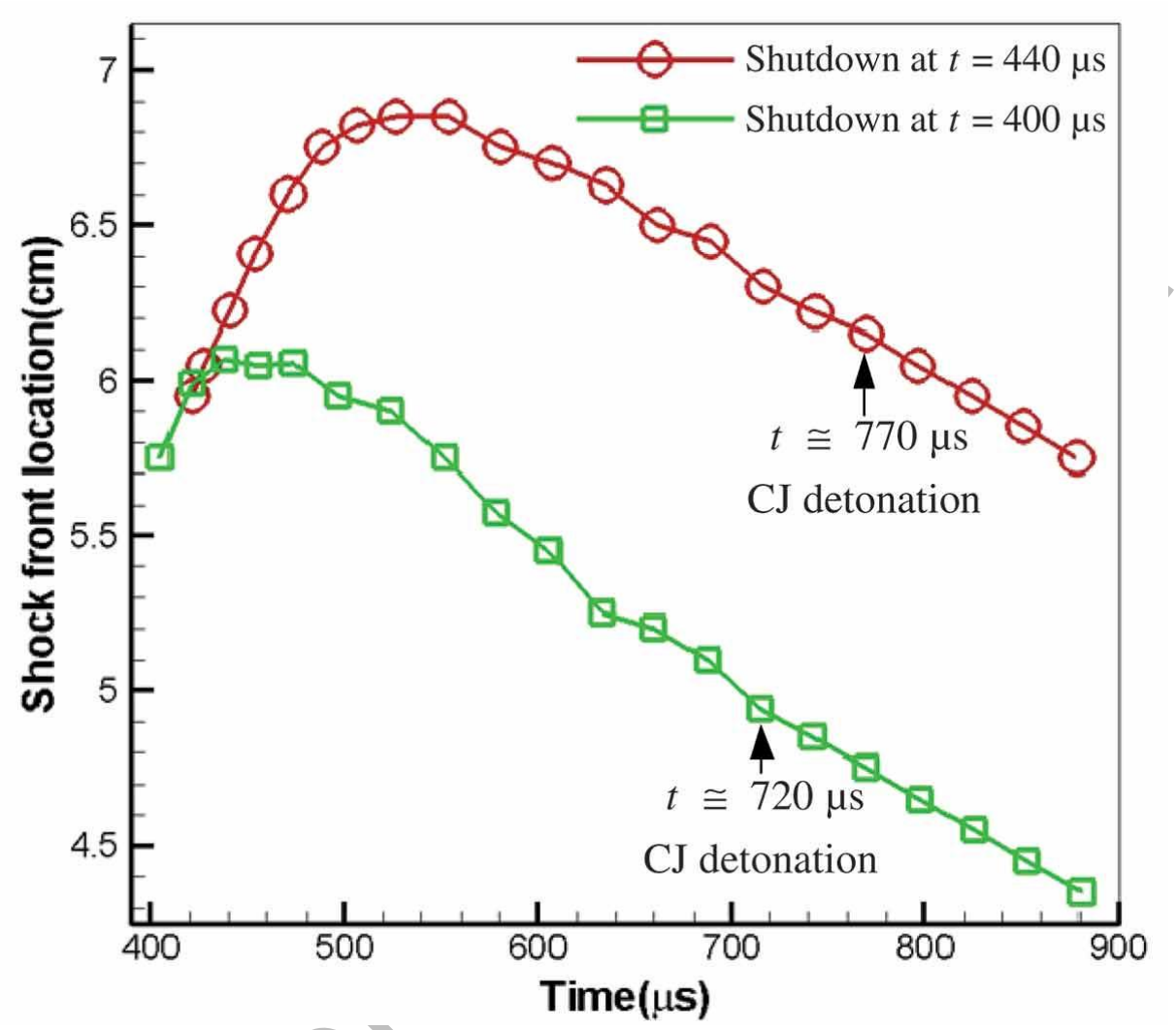

Fig.11 Contours of OH mass fraction and density schlieren images visualizing the stable CJ detonation in the supersonic combustible mixture, (a) t = 876.25 μs, (b) t = 881.65 μs.

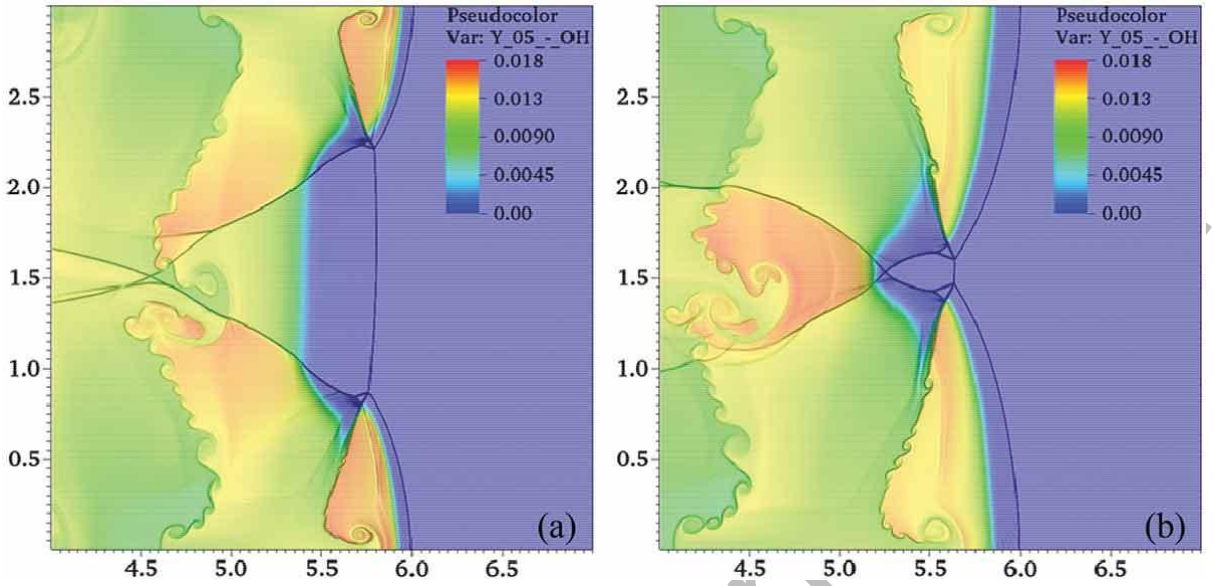

Fig.12 The shock front location for the whole process which is presented by four stages A, B, C and D. A: Overdriven detonation after the successful initiation; B: Attenuation from overdriven detonation to CJ detonation after the shutdown of the hot jet; C: Periodical Oscillations during the CJ detonation; D: Overdriven detonation after the re-injection of the hot jet.

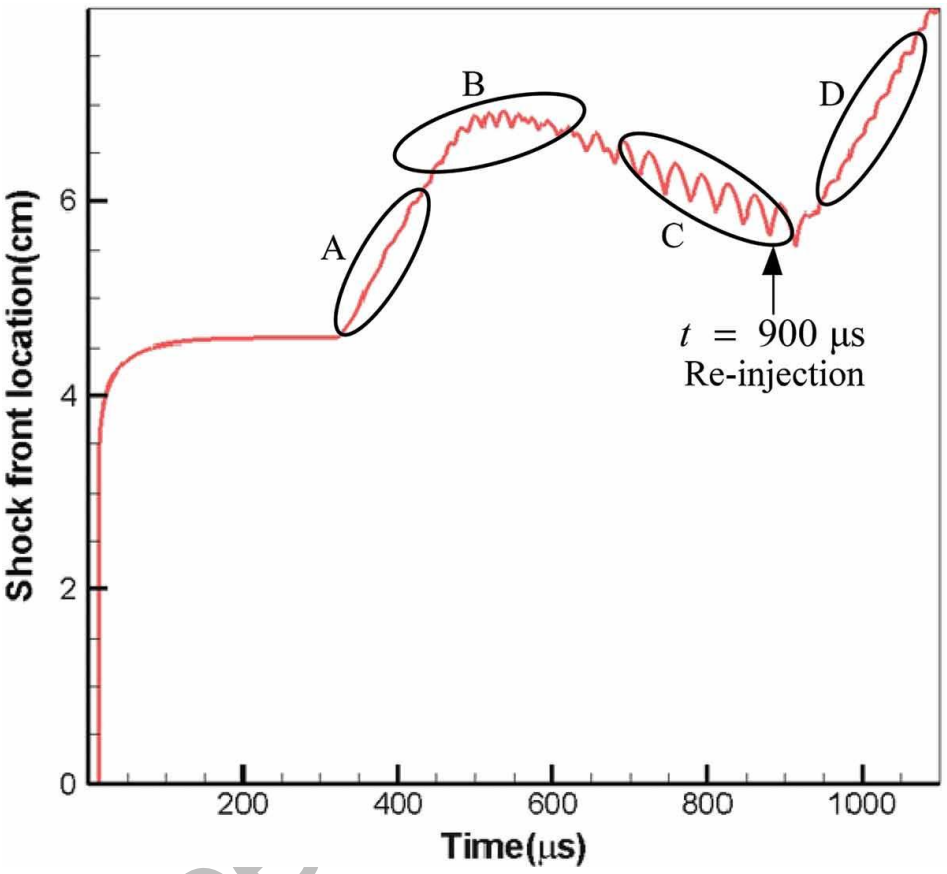

Fig.13 Distributions of three different kinds of mesh refinement: (a) four-level of $r_1 = 2,\ r_2 = 2,\ r_3 = 2$, (b) five-level of $r_1 = 2,\ r_2 = 2,\ r_3 = 2,\ r_4 = 2$, and (c) six-level of $r_1 = 2,\ r_2 = 2,\ r_3 = 2,\ r_4 = 2,\ r_5 = 2$

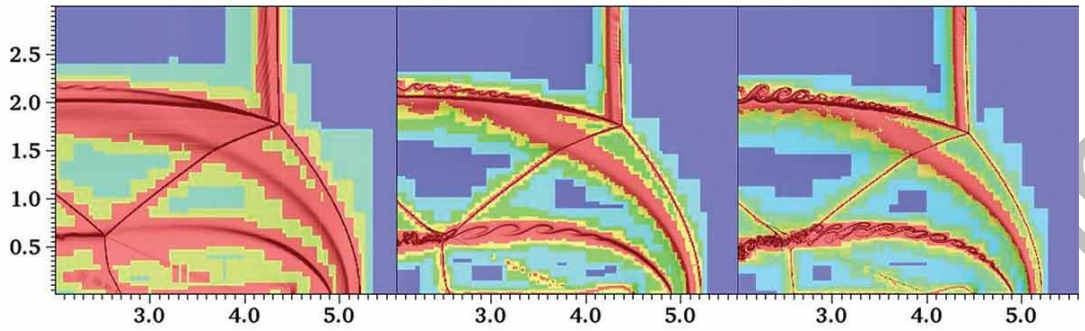

(a) Four-level refinement (b) Five-level refinement (c) Six-level refinement